THE INFLUENCE OF NANO-SiO₂ ON THE HYDRATION KINETICS OF PORTLAND CEMENT PASTE

JUN ZANG*, #WEIFENG LI*, **, XIAODONG SHEN*, **

*College of Materials Science and Engineering, Nanjing Tech University, Nanjing 210009, China
**State Key Laboratory of Materials-Oriented Chemical Engineering, Nanjing Tech University, Nanjing 210009, China

#E-mail: yc982@126.com (W.L.); xdshen@njtech.edu.cn (X.S.)

The hydration kinetics of Portland cement with and without nano-SiO₂ (NS) were evaluated via isothermal calorimetry and investigated based on the mathematic method of the Krstulovic-Dabic model in this paper. NS was used to substitute Portland cement at 0, 1 and 3 wt. % by mass. The test results obtained in this study indicated that the hydration process of Portland cement was dramatically promoted in terms of increasing the heat released and the heat release rate when NS was added. From the Krstulovic-Dabic model, the dynamics process of Portland cement was controlled by nucleation and crystal growth (NG), phase boundary interactions (I) and the diffusion (D) process, it does not matter whether there was NS or not, but the transformation of the controlling process occurred at a lower hydration degree for the NS-added pastes. Moreover, the increase in NS content increased the values of the kinetics parameters KNG and KI, but decreased KD and the reaction exponent to a different degree.

INTRODUCTION

The application of nanotechnology in the field of construction and building materials has received considerable attention recently, and it also seems to be a promising revolutionary tool towards the development of new classes of cementitious materials with outstanding properties [1-4]. A nano material, the product of nanotechnology, is defined as a very small particle with a size under the scale of 10^{-9} m [5]. Recent research indicated that most nano materials were found to show positive effects on the mechanical properties and durability of cement-based materials [6, 7] because of their unique physical and chemical properties [3, 5, 8].

A literature survey shows that nano-SiO₂ (NS) [9, 10], nano-TiO₂ (NT) [11], nano-Al₂O₃ (NA) [12, 13] carbon nanotubes (CNs) [14] and carbon nanofibres (CFs) [15, 16] are commonly used in cementitious systems. Among them, NS has received the greatest attention and has been investigated intensively. The experimental results have shown that the inclusion of NS in cement-based materials resulted in enhanced properties in terms of accelerating the cement hydration rate, refining the pore structure, improving the strength and increasing the durability [17-31].

Du et al [10] and Madani et al [18] reported that colloidal NS can significantly accelerate the rate of cement hydration, shorten the dormant period and reduce the setting times even with a low dosage due to its high surface. Similar results can also be observed in the previous research [17], in which powder NS particles were used. These promotion effects were attributed to the well distributed NS, which can serve as nucleation sites for the hydrated products to precipitate during cement hydration, thus increasing the hydration rate [17]. NS is also quite effective in modifying the microstructure of cement-based materials [21-23]. Due to its high pozzolanic reactivity [19, 20], NS can react with calcium hydroxide (CH) and produce an additional homogeneous C–S–H gel, leading to a denser microstructure of the hardened cementitious system. Meanwhile, the pozzolanic effect of NS is also contributing to reducing the size and the amount of the CH crystals arraying in the interfacial transition zone (ITZ) between the binding paste matrix and the aggregates, thus making the ITZ more compact [24, 25]. From some conducted experiments, the NS-added cement-based materials presented much superior mechanical properties [21, 26-28, 32]. Compared with the reference sample, the addition of 3 wt. % NS led to an increase in the compressive strength by 24 %, 8 % and 6.5 % at the age of 7, 28 and 90 days, respectively [33]. The mercury intrusion porosimetry (MIP) results also indicated the threshold pore size and the total porosity decreased significantly for the paste containing NS [29]. Meanwhile, these refined pore structures were advantageous for reducing the permeability considerably in terms of the calcium leaching rate and chloride ion penetration, resulting in improved durability [30, 31].

Until now, most researches have been focused on evaluating the modification effects of NS in Portland cement as well as the corresponding modification mechanism. However, there are scarcely any reports regarding quantifying the hydration kinetics of Portland cement containing NS, though many hydration kinetics models have been applied to other cementitious systems [34-40]. The hydration kinetics of cement determines the strength of the cement-based materials throughout their service life. Therefore, it is of great significance to understand the hydration kinetics of Portland cement with NS to help predicate and improve other properties.

Therefore, the objective of the present paper was to preliminarily study the hydration kinetics of Portland cement with NS based on the mathematic method of the Krstulovic-Dabic model [41]. Before this, an isothermal calorimeter was used to acquire the hydration heat evolution of the cement paste blended with NS. The methods used to determine the kinetics parameters have been detailly described in the published works [36, 42]. The results obtained in this study can help to provide a comprehensive understanding about the nanomodification effects of nanomaterials on cementitious systems.

The hydration kinetics method and the Krstulovic-Dabic model

The hydration kinetics model studies the reaction between cement and water from a dynamic point of view, and also analyses the influence of the reaction conditions on the reaction process during cement hydration, thus revealing the macroscopic and microscopic hydration mechanism [43]. Because of the complicated hydration mechanism between cement phases and water, the modified isothermal kinetics Equation 1 describing the heterogeneous system is acquired according to homogeneous reaction dynamics equation [40].

$$d\alpha/dt = Ae^{-E/RT} f(\alpha) \qquad (1)$$

where α, A, E, R, T, $f(\alpha)$, t are the reaction degree of the reactants, the pre-factor, the apparent activation energy, the gas constant, the thermodynamic temperature, the reaction mechanism function and reaction time, respectively.

The hydration degree is defined as the relative amount hydrated cement, resulting from the combined effects of the heat released by all the present phases. It can be expressed [36, 37] and calculated from the following equations:

$$\alpha_{(t)} = Q_t/Q_{max} \qquad (2)$$

$$d\alpha/dt = (dQ/dt)\cdot(1/Q_{max}) \qquad (3)$$

$$1/Q = 1/Q_{max} + t_{50}/Q_{max}\,(t - t_0) \qquad (4)$$

where Q_t and Q_{max} represents the accumulated hydration heat at time t and the ultimate total hydration heat

released of the sample. Normally, Q_{max} is often calculated with the help of Knudsen's extrapolation equations (Equation 4). In Equation 4, t refers to the time onset of the induction period while t_{50} represents the time when the hydration exothermic quantity reached half of the total heat of the hydration.

Usually, both the Tomosawa model and the Krstulovic-Dabic model are often utilised to evaluate the hydration kinetics of Portland cement [38]. However, compared with the Tomosawa model, the Krstulovic-Dabic model is more frequently used especially in acquiring the corresponding kinetic parameters in terms of the composite cementitious materials system. According to the Krstulovic-Dabic model [41], the cementitious materials' hydration can be assumed to be divided into three basic processes, namely nucleation and crystal growth (NG), phase boundary interactions (I) and a diffusion (D) process. The dynamics relationships between the hydration degree (α) and the reaction time (t) can be expressed in the integral form of Equations 5-7, while the corresponding differential form can be written as Equations 8-10, respectively. It is suggested that these three processes may simultaneously take place during the cement hydration process, and may occur alone or in pairs, but the reaction is controlled by the slowest one [37, 39].

$$[-\ln(1-\alpha)]^{1/n} = K_{NG}(t - t_0) \qquad (5)$$

$$[1 - (1-\alpha)^{1/3}]^1 = K_I(t - t_0) \qquad (6)$$

$$[1 - (1-\alpha)^{1/3}]^2 = K_D(t - t_0) \qquad (7)$$

$$[d\alpha/dt]_{NG} = K_{NG}\,n\,(1-\alpha)\,[-\ln(1-\alpha)]^{(n-1)/n} \qquad (8)$$

$$[d\alpha/dt]_I = K_I\,(1-\alpha)^{2/3} \qquad (9)$$

$$[d\alpha/dt]_D = 3K_D\,(1-\alpha)^{2/3}\,/\,2\,[1 - (1-\alpha)^{1/3}] \qquad (10)$$

where n is the reaction exponent. K_{NG}, K_I and K_D represent the rate constant for the hydration reaction process of NG, I and D, respectively.

Despite that there are some limitations existing in the Krstulovic-Dabic model, it is still considerably representative and easy to understand in the current academic sphere. The analysis result from this model does not only provide certain changes in the values of the kinetics parameters, but also conveniently gives a brief understanding about how the external factors influence cement hydration at each stage.

EXPERIMENTAL

Materials

A type II-52.5 Portland cement supplied from Jiangnan Onoda was used in this study. Its chemical composition and some physical properties are summarised in Table 1. A dry powder NS with an average particle size of 10 nm produced by Aladdin Industrial Corporation was used as the addition. Some parameters

Table 1. The physicochemical properties of the binder materials.

Oxides	Cement (%)	Nano-SiO$_2$ (%)
CaO	65.47	-
SiO$_2$	19.82	>99.5
Al$_2$O$_3$	4.66	–
SO$_3$	2.87	–
Fe$_2$O$_3$	3.03	–
MgO	0.84	–
K$_2$O	0.64	–
Na$_2$O	0.10	–
TiO$_2$	0.16	–
P$_2$O$_5$	–	–
Loss on ignition (LOI)	3.34	–
Density (g·cm^{-3})	3.2	2.08
Specific surface area (m^2·g^{-1})	0.355	270
Average particle size (nm)	23800	10
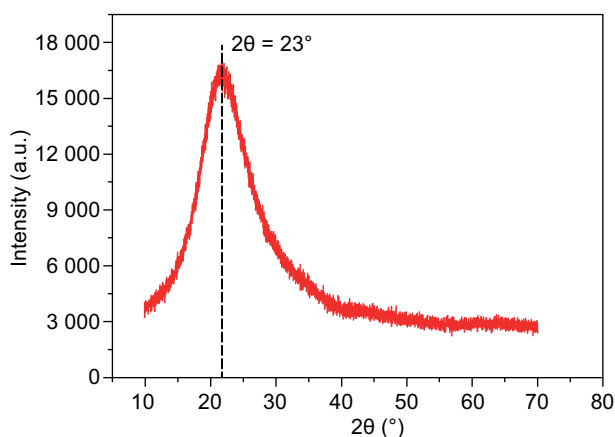
Figure 1. The X-ray diffraction pattern of NS.
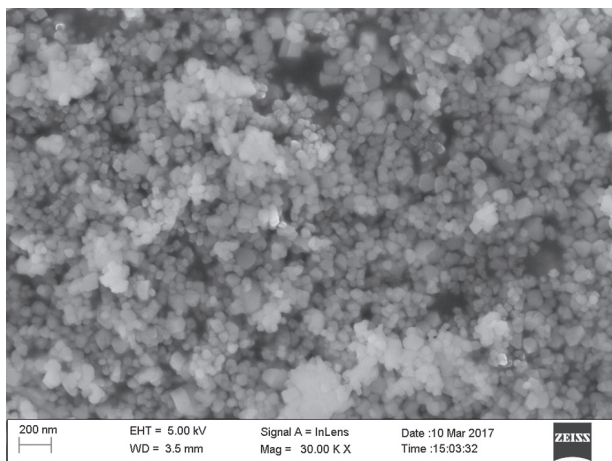
Figure 2. The FESEM micrograph of the NS powder (50 000 times magnification).

of the NS particles are also given in Table 1. The X-ray diffraction (XRD) pattern of the NS illustrated in Figure 1 confirms its amorphous nature. The field emission scanning electron microscopy (FESEM) (Figure 2) graph shows that the NS particle is round in shape, but seriously agglomerates. Moreover, the average particle size of the NS inferred from Figure 2 is about 15-20 nm. These properties are well in agreement with the data given in Table 1.

METHODS

The heat evolution during the cement hydration was performed using an 8-channel TAM Air (Thermometric AB, Sweden) isothermal calorimeter. Prior to the test, the NS and deionised water were conditioned under a constant temperature (20 °C) for 24 h to ensure the accuracy of the early age measurement. The replacement of NS in the cement was 1 % and 3 % by weight of cement, as shown in Table 2. For all mixtures, the water/solid (solid = Portland cement + NS) ratio was kept at 1. Because of its serious aggregation (from Figure 2), the NS was firstly dispersed in deionised water using sonication for 2 min to achieve relatively good dispersion. Then the cement was added and the mixtures were blended for another 2 min. During the test, around 10 g of this mixture was extracted and immediately injected into a sealed ampoule. The heat evolution was recorded at 20 °C over a period of 72 h.

Table 2. The investigated mixes.

Mix designation	Portland cement (g)	Nano-SiO$_2$ (g)	Deionised water (g)
N0	100	0	100
N1	99	1	100
N3	97	3	100

RESULTS AND DISCUSSION

The influence of NS on the heat evolution of Portland cement

The influence of NS on the heat evolution of the cement hydration is presented in Figure 3. The thermodynamics characteristic values of the hydration process including the end time of the induction period and total heat emission are summarised in Table 3. Like typical Portland cement [44, 45], the hydration behaviour of the control sample used in this experiment presents five stages: (I) Initial reaction period, (II) induction period, (III) acceleration period, (IV) deceleration period and (V) slow reaction period. Two peaks can also be observed. Both the initial dissolution of the phases and the early-stage reactions contribute to the

first peak in the initial reaction period. The second peak corresponding to the end of the acceleration period is mainly attributed to the hydration of tricalcium silicate (C$_3$S), during which C–S–H gels and CH are formed. Additionally, it is worth noting that a small "shoulder peak" formed right after the main hydration peak appeared and this peak is closely related to the renewed dissolution of tricalcium aluminate (C$_3$A) with the formation of ettringite (AFt).

As shown in Figure 3, the replacement of the cement by NS significantly changed the peak intensities or the time when they occurred without removing or adding additional peaks. The end time of the induction period t_0 for N0 was about 1.23 h while those of the N1 and N3 samples were about 1.02 h and 0.86 h (Table 3), respectively. In comparison with the control sample, the main peak occurred earlier when NS was added, especially for the sample with a higher amount of NS incorporated, indicating its acceleration effect on the C$_3$S hydration. The "shoulder peak" also shifted earlier in time for the NS–added samples. It means that the NS is conducive to the renewed dissolution of C$_3$A. Obviously, the NS powder also dramatically increased the peak intensities. All of these promotion effects were
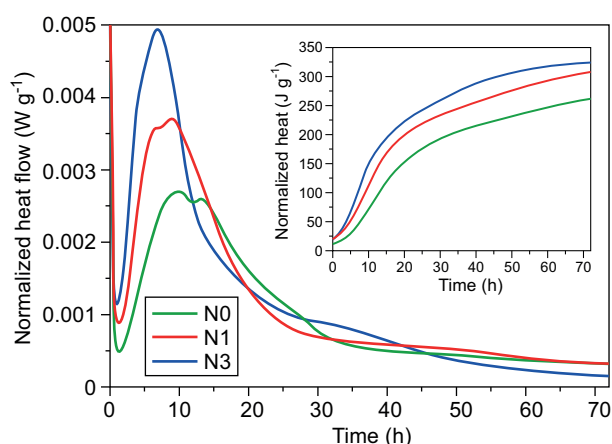
exhibited more significantly as the NS content increased from 1 % to 3 % though its increase was not in proportion to the increase of the heat release rate. Previous research presented that the increase in the acceleration was attributed to the fine NS particles working as additional nucleation sites, thus promoting the precipitation of the cement hydration products and the reaction process in the cement pastes [17].

Figure 3 also shows the cumulative heat released of the cement pastes blended with NS. The addition of NS increased the total heat released resulting from the acceleration of the cement hydration. The total hydration heat released of the three samples over 72 h were 261.69 J·g^{-1}, 307.55 J·g^{-1} and 324.74 J·g^{-1}, respectively. A similar acceleration effect of the NS on the cement hydration can also be observed in other research [10].

The influence of the NS on the hydration kinetics process of Portland cement

Table 4 summarises the kinetics parameters deduced in this study. By combining these kinetics parameters with Equations 8-10, the theoretical hydration rate curves of $d\alpha/dt\sim\alpha$, and the fitting curves of $F_{NG}(\alpha)$, $F_I(\alpha)$ and $F_D(\alpha)$ are obtained, as shown in Figures 4-6, respectively. It can be seen that the curves of $F_{NG}(\alpha)$, $F_I(\alpha)$ and $F_D(\alpha)$ for these three samples are well fitted to the theoretical $d\alpha/dt\sim\alpha$ curves though some simulation errors exist. The intersection points of α_1 and α_2 are turning points, indicating the hydration process transits from NG to I and from I to D, respectively. NG dominated at the early hydration stage when the hydration reaction degree was less than α_1, D controlled the later hydration stage when the hydration reaction degree was larger than α_2, while the middle hydration stage between α_1 and α_2 was controlled by the I process. It can be found that hydration kinetics process of the three samples all experienced NG, I and D processes, reflecting that all the samples have the same hydration reaction process controlled by the NG-I-D process. Though the reaction-controlled process did not change, the position of the intersection points, α_1 and α_2, obviously shifted when

Figure 3. The heat flow curves of the cement hydration with the NS addition.

Table 3. The thermodynamics characteristic values of the hydration process.

Sample	w/c	t_0 (h)	Q_{max} (J·g^{-1})	t_{50} (h)	Extrapolation equation
N0	0.5	1.23	328.95	28.22	1/Q = 0.00304 + 0.08578/(t-t0)
N1	0.5	1.02	342.47	16.63	1/Q = 0.00292 + 0.04855/(t-t0)
N3	0.5	0.86	389.11	16.01	1/Q = 0.00257 + 0.04114/(t-t0)

Table 4. The kinetic parameters of the hydration process of the cement with NS.

Sample	n	K$_{NG}$	K$_I$	K$_D$	Process	α_1	α_2
N0	1.24012	0.03643	0.01109	3.14324×10^{-3}	NG-I-D	0.1367	0.2962
N1	1.12811	0.04862	0.01339	2.35534×10^{-3}	NG-I-D	0.1026	0.2815
N3	1.02472	0.04929	0.01495	1.89928×10^{-3}	NG-I-D	0.0075	0.2196

the NS was incorporated when compared with the pure cement (Figures 4-6). Combined with Table 4, the values of α_1 decreased from 0.1367 to 0.1026 and the values of α_2 decreased from 0.2962 to 0.2815 after incorporating 1 % NS. When the dosage of NS increased from 1 % to

3 %, the values of α_1 continued to decrease from 0.1026 to 0.0075 along with value of α_2 decreasing from 0.2815 to 0.2196. All of these confirm that NS is conducive to shifting the transition of the controlling process at a lower hydration degree for the NS-added binder.

According to Table 4, the reaction exponent n also decreased with an increasing NS, indicating that NS greatly affected the crystal growth of the hydration products. The decrease in the reaction exponent might be attributed to the inherent properties of NS with high pozzolanic activity as well as the ultrafine particle size, conducing it to decrease the reaction resistance and significantly promoting the nucleation and crystal growth of the hydration products [9]. However, the change in the cement-NS system is different from that in the cement-fly ash system, in which the reaction exponent increased with an increase in the fly ash content [35]. As shown in Table 4, the values of K_{NG} and K_I increased with the increasing NS content. However, the increase degree was different. Because of its filler effects and high pozzolanic activity, the addition of NS in cement can result in a denser microstructure [24, 25]. That led to decreasing the effective diffusion coefficient K_D at the D process, which was opposite to the trend of K_{NG} and K_I. Obviously, during the overall hydration process, the coefficient for the NG process seemed about 3 ~ 4 times higher than that of the I process and 10 ~ 30 times higher than that of D process. The increase in the NS content increased the difference among these three processes. As discussed above, compared with the diffusion process, the higher NS incorporation exhibited greater influence on the chemical reaction process.

Figure 4. The hydration evolution curves for sample N0.
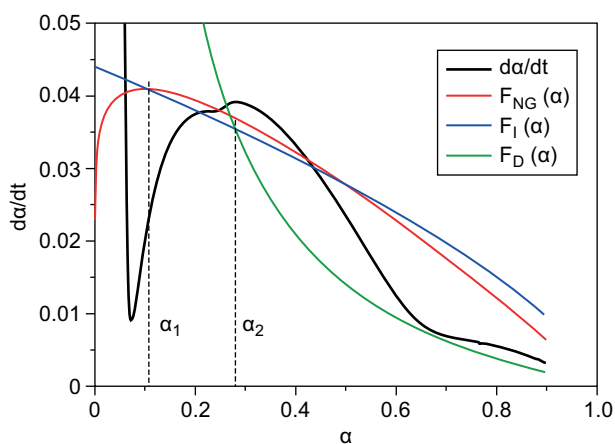
Figure 5. The hydration evolution curves for sample N1.
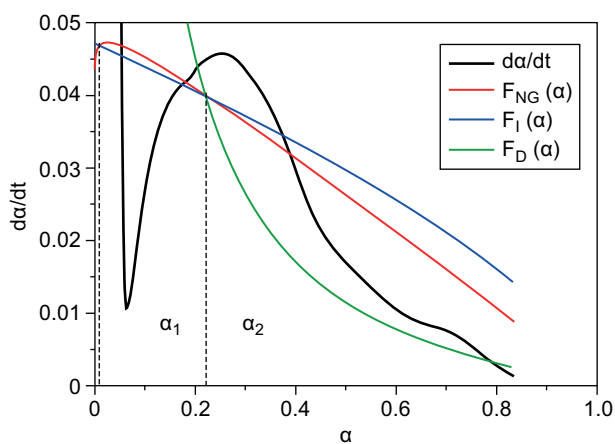
Figure 6. The hydration evolution curves for sample N3.

CONCLUSIONS

In this present work, the hydration kinetics of Portland cement with or without NS based on the mathematics method of the Krstulovic-Dabic model has been investigated. On the basis of the experimental study, the following conclusions have been derived:

● Adding NS dramatically accelerated the cement hydration process in terms of increasing the hydration rate and cumulative heat released;

● The model can determine the cement hydration process, which was controlled by the NG-I-D process. The addition of NS did not change the hydration process, but conduced it in shifting the transition of the controlling process at a lower hydration degree;

● Including NS in Portland cement decreased the values of the reaction exponent and K_D, but increased the values of the kinetics parameters K_{NG} and K_I to a different degree. Overall, NS exhibited a greater effect on the chemical reaction than diffusion.

Acknowledgements

REFERENCES

1. Park H., Jeong Y., Jun Y., Jeong J.-H., Oh J.E. (2016): Strength enhancement and pore-size refinement in clinker-free CaO-activated GGBFS systems through substitution with gypsum. Cement and Concrete Composites, 68, 57-65.doi: 10.1016/j.cemconcomp.2016.02.008

2. Sobolev K., Gutiérrez M.F. (2005): How nanotechnology can change the concrete world. American Ceramic Society Bulletin, 84(10), 14-18.

3. Sanchez F., Sobolev K. (2010): Nanotechnology in concrete – A review. Construction and Building Materials, 24(11), 2060-2071. doi: 10.1016/j.conbuildmat.2010.03.014

4. Hanus M.J., Harris A.T. (2013): Nanotechnology innovations for the construction industry. Progress in Materials Science, 58(7), 1056-1102. doi: 10.1016/j.pmatsci.2013.04.001

5. Motoyama Y., Appelbaum R., Parker R. (2011): The National Nanotechnology Initiative: Federal support for science and technology, or hidden industrial policy? Technology in Society, 33(1–2), 109-118. doi: 10.1016/j.techsoc.2011.03.010

6. Safiuddin M., Gonzalez M., Cao J.W., Tighe S.L. (2014): State-of-the-art report on use of nano-materials in concrete. International Journal of Pavement Engineering, 15(10), 940-949. doi: 10.1080/10298436.2014.893327

7. Kawashima S., Hou P., Corr D.J., Shah S.P. (2013): Modification of cement-based materials with nanoparticles. Cement and Concrete Composites, 36(0), 8-15. doi: 10.1016/j.cemconcomp.2012.06.012

8. Rashad A.M. (2013): Effects of ZnO₂, ZrO₂, Cu₂O₃, CuO, CaCO₃, SF, FA, cement and geothermal silica waste nanoparticles on properties of cementitious materials – A short guide for Civil Engineer. Construction and Building Materials, 48, 1120-1133. doi: 10.1016/j.conbuildmat.2013.06.083

9. Singh L.P., Karade S.R., Bhattacharyya S.K., Yousuf M.M., Ahalawat S. (2013): Beneficial role of nanosilica in cement based materials – A review. Construction and Building Materials, 47, 1069-1077. doi: 10.1016/j.conbuildmat.2013.05.052

10. Du H., Pang S.D. (2014). Effect of colloidal nano-silica on the mechanical and durability performances of mortar. in: 10th International Symposium on High Performance Concrete – Innovation and Utilization, HPC 2014, Beijing, China: Trans Tech Publications Ltd; 2015. pp. 443-448.

11. Zhang R., Cheng X., Hou P., Ye Z. (2015): Influences of nano-TiO₂ on the properties of cement-based materials: Hydration and drying shrinkage. Construction and Building Materials, 81(0), 35-41. doi: 10.1016/j.conbuildmat.2015.02.003

12. Barbhuiya S., Mukherjee S., Nikraz H. (2014): Effects of nano-Al₂O₃ on early-age microstructural properties of cement paste. Construction and Building Materials, 52, 189-193. doi: 10.1016/j.conbuildmat.2013.11.010

13. Nazari A., Sh R., Sh R., Shamekhi S.F., Khademno A. (2010): Influence of Al₂O₃ nanoparticles on the compressive strength and workability of blended concrete. Journal of American Science, 6(5), 6-9.

14. Konsta-Gdoutos M.S., Metaxa Z.S., Shah S.P. (2010): Highly dispersed carbon nanotube reinforced cement based materials. Cement and Concrete Research, 40(7), 1052-1059. doi: 10.1016/j.cemconres.2010.02.015

15. Brown L., Sanchez F. (2016): Influence of carbon nanofiber clustering on the chemo-mechanical behavior of cement pastes. Cement and Concrete Composites, 65, 101-109. doi: 10.1016/j.cemconcomp.2015.10.008

16. Metaxa Z.S., Konsta-Gdoutos M.S., Shah S.P. (2013): Carbon nanofiber cementitious composites: Effect of debulking procedure on dispersion and reinforcing efficiency. Cement and Concrete Composites, 36(0), 25-32. doi: 10.1016/ j.cemconcomp.2012.10.009

17. Senff L., Labrincha J.A., Ferreira V.M., Hotza D., Repette W.L. (2009): Effect of nano-silica on rheology and fresh properties of cement pastes and mortars. Construction and Building Materials, 23(7), 2487-2491. doi: 10.1016/j.conbuildmat.2009.02.005

18. Madani H., Bagheri A., Parhizkar T. (2012): The pozzolanic reactivity of monodispersed nanosilica hydrosols and their influence on the hydration characteristics of Portland cement. Cement and Concrete Research, 42(12), 1563-1570. doi: 10.1016/j.cemconres.2012.09.004

19. Gaitero J.J., Campillo I., Guerrero A. (2008): Reduction of the calcium leaching rate of cement paste by addition of silica nanoparticles. Cement and Concrete Research, 38(8), 1112-1118. doi: 10.1016/j.cemconres.2008.03.021

20. Hou P., Qian J., Cheng X., Shah S.P. (2015): Effects of the pozzolanic reactivity of nanoSiO₂ on cement-based materials. Cement and Concrete Composites, 55, 250-258. doi: 10.1016/j.cemconcomp.2014.09.014

21. Said A., Zeidan M.S., Bassuoni M., Tian Y. (2012): Properties of concrete incorporating nano-silica. Construction and Building Materials, 36, 838-844. doi: 10.1016/j.conbuildmat.2012.06.044

22. Aly M., Hashmi M.S.J., Olabi A.G., Messeiry M., Abadir E.F., Hussain A.I. (2012): Effect of colloidal nano-silica on the mechanical and physical behaviour of waste-glass cement mortar. Materials & Design. 33, 127-135. doi: 10.1016/j.matdes.2011.07.008

23. Liu J., Li Q., Xu S. (2015): Influence of nanoparticles on fluidity and mechanical properties of cement mortar. Construction and Building Materials, 101, 892-901. doi: 10.1016/j.conbuildmat.2015.10.149

24. Ji T. (2005): Preliminary study on the water permeability and microstructure of concrete incorporating nano-SiO₂. Cement and Concrete Research, 35(10), 1943-1947. doi: 10.1016/j.cemconres.2005.07.004

25. Monteiro P.J.M., Kirchheim A.P., Chae S., Fischer P., MacDowell A.A., Schaible E., et al. (2009): Characterizing the nano and micro structure of concrete to improve its durability. Cement and Concrete Composites, 31(8), 577-584. doi: 10.1016/j.cemconcomp.2008.12.007

26. Rong Z., Sun W., Xiao H., Jiang G. (2015): Effects of nano-SiO₂ particles on the mechanical and microstructural properties of ultra-high performance cementitious composites. Cement and Concrete Composites, 56, 25-31. doi: 10.1016/j.cemconcomp.2014.11.001

27. Gesoglu M., Güneyisi E., Asaad D.S., Muhyaddin G.F. (2016): Properties of low binder ultra-high performance cementitious composites: Comparison of nanosilica and microsilica. Construction and Building Materials, 102, 706-713. doi: 10.1016/j.conbuildmat.2015.11.020

28. Nazari A., Riahi S. (2011): Splitting tensile strength of concrete using ground granulated blast furnace slag and SiO2 nanoparticles as binder. Energy and Buildings, 43(4), 864-872. doi: 10.1016/j.enbuild.2010.12.006

29. Tanaka K., Kurumisawa K. (2002): Development of technique for observing pores in hardened cement paste. Cement and Concrete Research, 32(9), 1435-1441. doi: 10.1016/S0008-8846(02)00806-2

30. Kong D., Du X., Wei S., Zhang H., Yang Y., Shah S.P. (2012): Influence of nano-silica agglomeration on microstructure and properties of the hardened cement-based materials. Construction and Building Materials, 37, 707-715. doi: 10.1016/j.conbuildmat.2012.08.006

31. He X., Shi X. (2008): Chloride permeability and microstructure of Portland cement mortars incorporating nanomaterials. Transportation Research Record: Journal of the Transportation Research Board, 2070(1), 13-21. doi: 10.3141/2070-03

32. Shaikh F.U.A., Supit S.W.M. (2015): Chloride induced corrosion durability of high volume fly ash concretes containing nano particles. Construction and Building Materials, 99, 208-225. doi: 10.1016/j.conbuildmat.2015.09.030

33. Ghafari E., Costa H., Julio E., Portugal A., Duraes L. (2014): The effect of nanosilica addition on flowability, strength and transport properties of ultra high performance concrete. Materials & Design, 59, 1-9. doi: 10.1016/j.matdes.2014.02.051

34. Zhu B.Q., Song Y.N., Li X.C., Chen P.A., Ma Z. (2015): Synthesis and hydration kinetics of calcium aluminate cement with micro MgAl₂O₄ spinels. Materials Chemistry and Physics, 154, 158-163. doi: 10.1016/j.matchemphys.2015.01.060

35. Han F., Zhang Z., Liu J., Yan P. (2016): Hydration kinetics of composite binder containing fly ash at different temperatures. Journal of Thermal Analysis and Calorimetry, 124(3), 1691-1703. doi: 10.1007/s10973-016-5295-z

36. Zhang N., Li H.X., Zhao Y.Z., Liu X.M. (2016): Hydration characteristics and environmental friendly performance of a cementitious material composed of calcium silicate slag. Journal of hazardous materials, 306, 67-76. doi: 10.1016/j.jhazmat.2015.11.055

37. Chang X.L., Yang X.P., Zhou W., Xie G.S., Liu S.H. (2015): Influence of Glass Powder on Hydration Kinetics of Composite Cementitious Materials. Advances in Materials Science and Engineering, 713415, 1-7. doi: 10.1155/2015/713415

38. Thomas J.J., Biernacki J.J., Bullard J.W., Bishnoi S., Dolado J.S., Scherer G.W. et al. (2011): Modeling and simulation of cement hydration kinetics and microstructure development. Cement and Concrete Research, 41(12), 1257-1278. doi: 10.1016/j.cemconres.2010.10.004

39. Liu S.H., Wang L., Gao Y.X., Yu B.Y., Tang W. (2015): Influence of fineness on hydration kinetics of supersulfated cement. Thermochimica Acta, 605, 37-42. doi: 10.1016/j.tca.2015.02.013

40. Yan P., Zheng F. (2006): Kinetic Model for the Hydration Mechanism of Cementitious Materials. Journal of the Chinese Ceramic Society, 34(5), 555.

41. Krstulović R., Dabić P. (2000): A conceptual model of the cement hydration process. Cement and Concrete Research, 30(5), 693-698. doi: 10.1016/S0008-8846(00)00231-3

42. Han F., Zhang Z., Wang D., Yan P. (2015): Hydration kinetics of composite binder containing slag at different temperatures. Journal of Thermal Analysis and Calorimetry, 121(2), 815-827. doi: 10.1007/s10973-015-4631-z

43. Zhao X. (1984). Principle of Chemical Reaction Dynamics (in Chinese). Beijing, High education Press.

44. Bullard J.W., Jennings H.M., Livingston R.A., Nonat A., Scherer G.W. Schweitzer J.S. et al. (2011): Mechanisms of cement hydration. *Cement and Concrete Research*, 41(12), 1208-1223. doi: 10.1016/j.cemconres.2010.09.011

45. Taylor H.F. (1997). *Cement chemistry*. Thomas Telford.